Fluorescent imaging for cancer therapy and cancer gene therapy

Yanghee Woo,[1] Shyambabu Chaurasiya,[1] Michael O'Leary,[1] Ernest Han,[1] and Yuman Fong[1]

[1]Department of Surgery, City of Hope Medical Center, 1500 East Duarte Road, Duarte, CA 91010, USA

The translation of laboratory science into effective clinical cancer therapy is gaining momentum more rapidly than any other time in history. Understanding cancer cell-surface receptors, cancer cell growth, and cancer metabolic pathways has led to many promising molecular-targeted therapies and cancer gene therapies. These same targets may also be exploited for optical imaging of cancer. Theoretically, any antibody or small molecule targeting cancer can be labeled with bioluminescent or fluorescent agents. In the laboratory setting, fluorescence imaging (FI) and bioluminescence imaging (BLI) have long been used in preclinical research for quantification of tumor bulk, assessment of targeting of tumors by experimental agents, and discrimination between primary and secondary effects of cancer treatments. Many of these laboratory techniques are now moving to clinical trials. Imageable engineered fluorescent probes that are highly specific for cancer are being advanced. This will allow for the identification of tumors for staging, tracking novel therapeutic agents, assisting in adequate surgical resection, and allowing image-guided biopsies. The critical components of FI include (1) a fluorescent protein that is biologically safe, stable, and distinctly visible with a high target to background ratio and (2) highly sensitive optical detectors. This review will summarize the most promising optical imaging agents and detection devices for cancer clinical research and clinical care.

INTRODUCTION

Traditional imaging modalities in clinical practice are used to identify pathology in relation to anatomy. Computed tomography (CT), magnetic resonance imaging (MRI), or positron emission tomography (PET) are useful diagnostic or surveillance tools. Until recently, imaging was not used to identify targets for therapy and quantify the real-time effectiveness of therapy. Recent advances in biological imaging now allow quantification of targets for therapeutic agents. For example, the binding of radioactive antibodies to the human epidermal growth factor receptor-2 (HER-2) has been tested for the ability to identify and quantify the level of HER-2 expression for targeting by Herceptin.[1] Furthering this concept, radioactively tagged check-point inhibitors have been used to quantify on- and off-target binding by antibodies.[2]

In novel cancer therapies, there are three imaging needs: (1) imaging for agent/vector distribution to correlate to the effectiveness of therapy, (2) imaging of off-target agent/vector distribution to correlate with toxicity, and (3) imaging of immune cell infiltration to discriminate direct agent/vector effectiveness from the effectiveness of a secondary immune response. Many recent studies of nuclear medicine-based biological imaging offer potential clinical translation of these three areas to trials and future therapy. Other papers in this special issue review these.

Non-white light optical imaging techniques include bioluminescent imaging (BLI) and fluorescent imaging (FI). In the laboratory and preclinical realms, bioluminescent and fluorescent techniques have been invaluable. Most BLI requires substrates that are activated for luminescence. Because these would be considered drugs in clinical development, most BLI has been restricted to the preclinical area and will not be discussed in detail here. In the current review, we summarize the use of FI in cancer and gene therapy. Recent progress in hardware development now provides for clinical machines to detect real-time *in vivo* fluorescence in humans. We will first review the approaches being tested in cancer therapy outside of gene therapy. We will then summarize the potential use of such optical imaging techniques in gene therapy that have reached human trials and future prospects (Table 1).

FLUOROPHORES

There are many advantages to FI. FI is real-time imaging and does not require ionizing radiation[3] and requires no substrate for light emission.[4] It allows simultaneous detection of multiple cellular processes using multiple emission spectrums (colors) of fluorophores. Many fluorescent molecules are available for laboratory and clinical use. In general, fluorophores exist that fluoresce green (emission wavelength ~500 nm), orange (emission at 550–570 nm), red (red fluorescent protein [RFP]; emission at 570–620 nm), and far-red (emission at over 620 nm).

The three most commonly used near-infrared (NIR) fluorophores routinely in clinical use today are methylene blue,[5] fluorescein (FL),[6] and indocyanine green (ICG). Their excitation and emission characteristics are summarized in Table 2. The most common use of these agents is for the demonstration of organ perfusion. Their

Table 1. Applications of fluorescent imaging for cancer and cancer gene therapy

Therapy	Application
Cancer therapy	delineating tumors and margins
	mapping lymphatics
	identification of metastases
	identification of vital anatomic structures
Cancer gene therapy	tracking oncolytic viruses
	tracking immune cells

Table 2. Common fluorophores in clinical testing and use

Fluorophore	Excitation wavelength (nm)	Emission wavelength (nm)
Fluorescein sodium	475—490	510—520
Methylene blue	550—700	690
Indocyanine green (ICG)	740—800	800—860

characteristics *in vivo* depend upon the injected dose, biodistribution, clearance, metabolism, and affinity targeting.[7] The preclinical use in quantifying gene expression has become commonplace. ICG was approved as a clinical agent in 1959 and is used in applications as diverse as determining cardiac output, determining hepatic function and liver blood flow, and ophthalmic angiography. ICG offers a high signal-to-background ratio (SBR) due to low autofluorescence and high tissue penetration at a wavelength of 820 nm, distinct from the wavelengths absorbed by blood and skin. ICG has a half-life of 150—180 s and is cleared by the liver. It is a very safe clinical agent with only rare adverse events (AEs). Hypersensitivity reactions rarely occur (1:40,000 administrations).[8]

Green fluorescent protein (GFP), discovered in 1962 by Shimomura et al., is the most studied fluorophore in molecular therapy. GFP is a relatively small nontoxic protein consisting of 238 amino acids and weighing 27 kDa. It is derived from *Aequorea victoria* and was first sequenced in 1992.[9] GFP gene can be placed into an expression cassette and cloned into a virus or a cell for tracking viral or cellular therapy.

SUMMARY OF DEVICES USED IN FLUOROSCOPY

Many FI devices exist for both laboratory and clinical use (Table 3). They, in general, are composed of a light source, usually with a variety of wavelengths. Filters are inserted to eliminate excitation and ambient light for use with one or more fluorophores. Detector(s) of the appropriate spectral range and sensitivity, along with a good display for real-time fluorescent readout superimposed on a reference image, are also essential. The device architecture needs to consider the desired field of view, resolution, and excitation/emission wavelengths. The architecture of probes and detectors also needs to accommodate the specific clinical application: open surgery, laparoscopic, thoracoscopic, endoscopic, and robot-assisted procedures.

There are several commercially available devices for intraoperative NIR fluorescence (NIRF) imaging.[10] The most popular are the Firefly (Intuitive Surgical, Sunnyvale, CA, USA), SPY-PHI and Pinpoint Imagers (Stryker, Kalamazoo, MI, USA), and EleVision platform (Medtronic, Dublin, Ireland). Several systems are also made to work on surgical microscopes, including the FL800 (Leica Camera, Wetzlar, Germany) and Infrared 800 (Carl Zeiss AG, Oberkochen, Germany).

FLUORESCENT GUIDANCE IN CANCER SURGERY

Several fluorescent dyes are used in clinical medicine, with the most popular being FL, methylene blue, and ICG (Table 2). The most common uses have been for the assessment of perfusion. The fluorescence generated by the dye allows a significant increase of contrast between well-perfused areas and poorly diffused areas. By injecting the dyes, vascular and general surgeons have assessed organ perfusion in patients with vascular disease, and plastic surgeons have used FI to assess the viability of microvascular flaps. In open surgery, many inexpensive handheld devices are available for the assessment of blood flow. All of these fluorescent dyes can be used to look at organ or tissue flap blood flow.[11]

Recent years have seen a proliferation of devices (Table 3) for the clinical detection of fluorescence in endoscopy, laparoscopy, and thoracoscopy. These allow the use of fluorescence for perfusion assessment in minimally invasive procedures. The utility of laparoscopic ICG perfusion assessment is used to evaluate colonic perfusion to allow well-perfused anastomosis after resection of the colon for cancer.[12] The use of ICG perfusion also enables well-perfused ureters in reconstruction after bladder cancer resection to improve outcomes.[13] Real-time ICG angiography with the SPY FI platform (Stryker, Kalamazoo, MI, USA) decreases ureter enteric strictures in urinary diversions performed during radical cystectomy (SPY guided: 0/93 ureters, 0%; non-SPY guided: 7/93 ureters, 7.5%; p = 0.01).

Flow-based tumor identification

More recently, these fluorescent dyes have also been used to highlight tumors based on the high blood flow of tumors. A whole literature has emerged in resection of neurologic tumors using FL-guided surgery (FGS). Sodium FL enhances margin-free resections of spinal gliomas surgery[14] and brain neoplasms[15] by enhancing delineation of tumor margins. Methylene blue and NIRF have also been used successfully to identify thyroid and parathyroid tumors.[16]

The use of ICG fluorescence for the identification of tumors relies on a slightly different principle. Within minutes of ICG injection, the liver will become fluorescent green because of dye metabolism. Tumors within the liver stay non-fluorescent for over 1 h. During that first hour, fluorescent dye will also be excreted by the liver into the biliary system, allowing identification of the major bile ducts. Liver surgeons rely on the differential fluorescence of liver and tumor and the outlining of bile ducts for safe, margin-free resection of liver cancers (Figure 1).[17]

Table 3. Names, types, and manufacturers for approved near-infrared fluorescence imaging devices for use in surgery

Name	Manufacturer	Modality
SPY-PHY	Stryker	handheld
SPY Pinpoint	Stryker	laparoscopic/endoscopic
SPY Elite	Stryker	stand alone/open air
EleVision	Medtronic	stand alone/laparoscopic/endoscopic
Opal1	Karl Storz	laparoscopic/endoscopic
Firefly	Intuitive Surgical	robotic
pde-neoII	Hamamatsu	handheld
Fluobeam	Fluoptics	handheld
FL800	Leica Camera	surgical microscope
Infrared 800	Carl Zeiss AG	surgical microscope
Spectrum	Quest	stand alone/open air

Figure 1. Use of ICG for delineation of tumor margin _in vivo_

ICG is injected intravenously in patients. The liver metabolizes the fluorophore and turns fluorescent green. Tumors in the liver remain dark, and margins can be seen as negative if they are fluorescent green. (A) White light display of the tumor in the liver. (B) The delineation by ICG fluorescence. (C) The cut liver edge by white light. (D) Fluorescent display shows the negative margin since the entire surface is fluorescent.
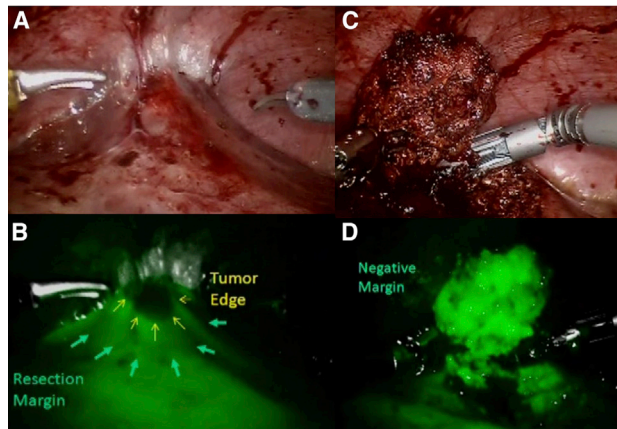
Sentinel lymph node mapping for cancer

Many cancers, including breast, colon, and skin cancers, spread to lymph nodes. Such lymphatic spread has significant prognostic and therapeutic implications. Those patients with lymphatic metastases have poorer survival and usually benefit from excision of the affected lymphatic tissues. Identification of lymphatic flow is, therefore, one of the primary goals of surgical care.

Fluorescent dyes have been long used in this endeavor. The dye is injected near the primary tumor, fluorescence detection then identifies the first group of nodes to which the lymph travels. These lymph nodes are called sentinel lymph nodes and biopsied as the most likely to have cancer. In a recent meta-analysis of 18 sentinel lymph node studies using methylene blue dye alone in patients with breast cancer, the combined identification rate was 91%, with pooled sensitivity, negative predictive value, and an accuracy rate of 87%, 91%, and 94%, respectively. Thus, mapping with this inexpensive dye using inexpensive equipment can provide important clinical information in the care of breast cancer patients.

NIRF imaging after peritumoral injection of ICG in patients with stomach cancer undergoing radical gastrectomy has been found to provide surgeons with effective visualization of the lymphatic anatomy of D2 lymph node stations to ensure clearance of tumor-draining basins. Lymph node retrieval was higher in yield when NIRF was used as a guide than in the historical controls (48.9 versus 35.2; p < 0.001). All positive lymph nodes were green, but not all green nodes were positive. These findings suggested that fluorescent lymphography may assist the surgeon to intraoperatively identify and retrieve all necessary lymph nodes in real time to achieve a more thorough lymphadenectomy.[18]

ICG mapping for lymphatic obstruction

An emerging clinical use of fluorescence-guided therapy for cancer is ICG mapping of lymphatics. Many patients who have cancer surgery develop lymphedema, swelling of extremities near areas of sites of surgery due to destruction of lymphatics. Lymphatic bypasses are emerging as an essential therapeutic procedure to reduce morbidity and improve quality of life. ICG-assisted lymphatic mapping has proven invaluable in the surgical execution of these bypasses that will enhance the quality of life.[19]

SPECIFIC FLUORESCENT AGENTS FOR LOCALIZATION OF CANCER

All of the fluorescent techniques above rely on blood and lymph flow. There is also a push academically and industrially to develop fluorescent agents for the specific identification of cancer. The most advanced fluorescent agents for tumor localization are listed in Tables 2 and 4. They fall into two categories: antibodies or ligands for proteins and receptors on cancer cell surfaces and substrates for cancer-specific metabolic pathways. Almost all of these are labeled with either ICG or one of the cyanine red dyes, including Cy5, Cy5.5, and Cy 7.0. ICG-based compounds are very attractive because they can be detected in many of the currently available fluorescent-detection hardware already in operating rooms (Table 3). With minor modifications, this equipment can also detect cyanines and other NIRF dyes.

Fluorescent substrates for cancer-specific pathways
Cathepsin-based imaging

The protease cathepsin is secreted by cancer cells at a higher level than healthy cells. It is thought that tumors activate cathepsins to alter the tumor microenvironment for cancer growth and metastasis. Two agents under clinical investigations for cathepsin-based imaging of cancer are LUM015 from Lumicell and VGT-309 from Vergent.

LUM015 is an imaging probe that is activated in the presence of cathepsins. It is labeled with Cy5 and allows FI _in vivo_ to assess tumor

Table 4. Some fluorescent compounds in clinical development for use in cancer diagnosis and therapy

Compound	Target	Dye	Application	Clinical	Excitation/emission	Company
LUM015	cathepsin	Cy5	breast cancer and sarcoma resection margins	phase 2	630/675 nm	Lumicell
VGT-309	cathepsin	ICG	multi-tumor identification	phase 1	745/820 nm	Vergent
AVB-620	MMP-9	Cy5 + Cy7	multi-tumor identification	phase 2	630/620−850 nm	Avelas Biosciences
C-Dots	integrin	Cy5.5	breast and head and neck cancers; margins and LN mapping	phase 2	630/710 nm	Elucida Oncology
BLZ-100	chlorotoxin	ICG	brain, breast, skin cancer identification	phase 1	745/820 nm	Blaze Bioscience
LN, lymph node.						

margins at surgery using the LUM Imaging System (Lumicell, Wellesley, MA, USA). Smith et al.[20] studied the use of LUM015 in breast cancer patients in a phase 1 trial. It was found to be safe and cleaved as expected in tumors.[20] The tumor was distinguished from normal tissue in pre- and post-menopausal women, and readings were not affected by breast density. The favorable biodistribution and pharmacokinetics seen have led to current ongoing trials in breast cancer and sarcoma.

VGT-309 is another cathepsin imaging probe. Cathepsins X, B/L, and S specifically activated the probe. This compound has an ICG molecule integrated along with a quencher for fluorescence. When this molecule is exposed to cathepsin, the quencher is cleaved, allowing detection of the fluorescent ICG. Because ICG detection already has approved clinical-detection hardware, many clinical imaging systems already exist in hospitals for trials and hopefully in the future for clinical use. In preclinical studies, Suurs et al.[21] studied FI in BALB/c mice bearing a murine breast tumor. FI revealed an increased tumor-to-background contrast over time up to 15.1, 24 h post-probe injection.[21] This agent has gone through phase 1 healthy volunteer trials and is entering into cancer patient phase 1/2 trials.

Matrix metalloproteinase (MMP) imaging

MMPs are proteins that break down extracellular matrix proteins during physiologic tissue remodeling. They are secreted in an inactive form and are activated by extracellular proteinases. These proteins, and in particular MMP-3, are thought to be involved in tumor initiation. MMP-3 activity is high in many types of cancers. The protease-activatable FI agent, AVB-620, was designed to image breast and other tumors. Labeling by Cy5 and Cy7 allows detection of AVB-620 by fluorescence detection.[22] MMPs hydrolyze AVB-620, triggering tissue retention and a ratiometric fluorescence color change visualized using camera systems capable of imaging fluorescence and white light simultaneously. Miampamba et al.[22] performed an *ex vivo* human tumor study on the biological activity of this agent. Patient tumor tissue and healthy adjacent breast tissue were homogenized and incubated with AVB-620, and fluorogenic responses were compared. Tumor tissue had 2- to 3-fold faster hydrolysis than matched healthy breast tissue, generating an assay sensitivity of 96% and specificity of 88%.[22] AVB-620 is now in human phase 1/2 trials.

Fluorescent nanoparticle imaging

The need for imaging cancer-infiltrated lymph nodes has fueled the development of many other platforms to aid in the accurate identification of tumor-bearing lymph nodes. Ultrasmall tumor-targeting inorganic (silica) nanoparticles are one of several promising cancer-imaging probes. C-Dots from Elucida Oncology, labeled with Cy5.5 for fluorescent detection, have been advanced into phase 2 trials for cancerous lymph node detection in breast cancer and head and neck cancer.[23]

Chlorotoxin (CTX)-based agents

An exciting class of agents entering clinical trials relies on peptide conjugates with natural tumor-binding qualities derived from the venom of the scorpion *Leiurus quinquestriatus*. These agents can bind to several cancers, including gliomas and a variety of other solid tumors. BLZ-100 is one such agent and uses ICG as the fluorophore.[24] Baik et al.[24] recently reported the preclinical testing of this agent in the identification of head and neck squamous cell carcinoma (HNSCC). In HNSCC xenografts, BLZ-100 proved to be a sensitive and specific marker of HNSCC and could distinguish high-risk from low-risk dysplasia.[24] BLZ-100 is being moved forward through human testing.

Fluorescent antibody-based imaging

Many cell-surface tumor markers have been useful for the pathologic diagnosis of solid tumors. Of these, the most important have been the following: (1) carcinoembryonic antigen (CEA) for colorectal cancer, breast cancer, lung cancer, and gastric cancer; (2) prostate-specific membrane antigen (PSMA) for prostate cancer; and (3) cancer antigen (CA125) for ovarian cancer. Specific, high-affinity antibodies have been developed and brought into the diagnostic imaging realm for these and other cancers. As such, [124]I-CEA antibody PET scanning[25] and ^{68}Ga-PSMA antibody PET scanning[26] are highly promising clinical imaging techniques. Some of these antibodies are now also being labeled with fluorophores and brought forth as possible operative and procedural imaging modalities. We will restrict our remarks to CEA antibodies in this review. Many other antibodies, including ones directed at PSMA, Tag-72, are under testing.

CEA antibodies

CEA is a non-internalizing tumor antigen expressed at high levels in many tumors, including colorectal cancer (90%), gastric cancer (80%), pancreatic cancer (60%), breast cancer (50%), and lung cancer
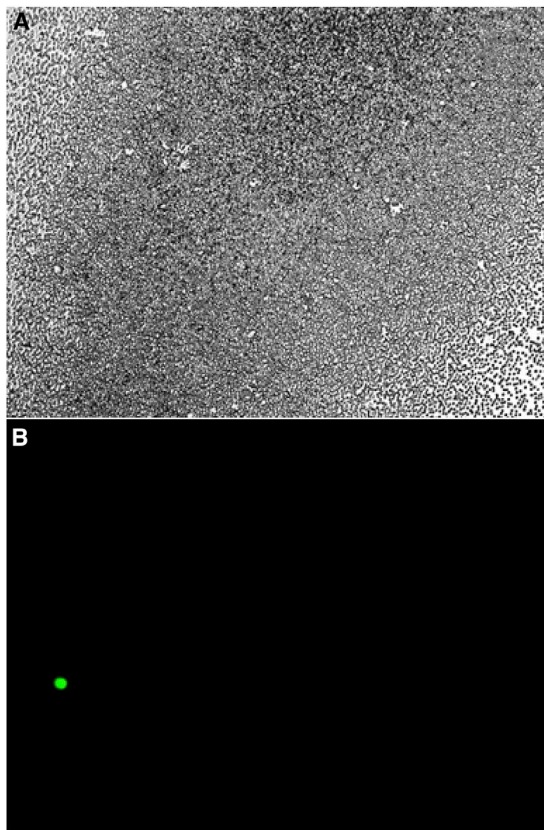
Figure 2. Sensitive detection of cancer cells using cancer-specific fluorescent oncolytic viruses

Liver cancer cells are combined with various amounts of benign hepatocytes. Shown is a mixture of 1:2,000,000 cancer:benign cells. White light microscopy is shown (A); fluorescent microscopy is shown (B). Sensitivity of detection by routine cytology is one cancer cell in the background of 20,000 normal cells.

(60%).[27–31] The first example of an anti-CEA monoclonal antibody (mAb) for FGS in the clinic is SGM-101 (SurgiMab), a chimeric anti-CEA mAb-IR700 evaluated in 12 pancreatic cancer patients and shown to be safe and feasible.[32–34] A significant disadvantage of this agent is the potential for human anti-chimeric antibody (HACA) response and the lack of clinically available instruments to image at 700 nm wavelength. Therefore, Yazaki et al.[35] have developed a novel antibody-tagged fluorophore, anti-CEA-M5A-IR800, that combines a humanized mAb against CEA (M5A mAb) with an IR-800 dye that is detectable by currently available clinical imaging systems. The anti-CEA M5A-IR800 conjugate can rapidly and effectively image colon cancer[36] as well as pancreatic cancer[37,38] in mouse patient-derived orthotopic xenograft (PDOX) models.[39]

OPTICAL IMAGING OF ONCOLYTIC VIRAL THERAPY

Some of the most robust examples of the preclinical *in vivo* research that use FI technology with active cancer targeting are in oncolytic viral therapy. The field of oncolytic viral therapy aims to design viruses that specifically infect and kill cancer and generate an immune response directed at cancer. By having the virus carry a transgene coding a fluorescent protein, FI allows documentation of sites of infection and replication. It can also allow assessment of therapeutic viral delivery to correlate with on-target efficacy and off-target toxicities. Thus, there is much data that FI can be used to track oncolytic viral therapy.

In preclinical studies, oncolytic viruses (OVs) that encode EGFP also hold promise for enhancing the diagnosis and staging of cancer. By injection of replication-competent OVs such as vaccinia virus, herpes simplex virus 1 (HSV-1), and Newcastle viruses that express EGFP, investigators have been able to use optical imaging of EGFP expression to identify tumors in their organs of origin, distant sites of metastases including the lymph nodes[40] and peritoneum,[41] and tumor involvement of nerves.[42]

In animal models, virally guided cancer detection has been used to guide cancer surgery.[43] NV1066 is a novel oncolytic herpes viral strain that specifically infects cancer cells and expresses GFP. An *in vivo* breast cancer metastasis model was treated with NV1066 via injection into the primary tumor. Axillary lymph nodes were tracked using an *in vivo* FI system, and tumors were successfully identified in the axillary lymph node by NV1066 infection and expression of EGFP. Histologic and molecular assessment of GFP-positive lymph nodes confirmed positive metastases identification. This demonstrated that optical imaging could track viral infection of primary breast tumors to enable real-time intraoperative detection and resection of lymphatic metastases.

In another animal study, NV1066 allowed real-time optical imaging of fluorescent proteins in OV-infected peritoneal cancers to enable detection and clearance of occult peritoneal metastases.[41] In *in vivo* models of mice with human gastric cancer cells implanted into the peritoneum, NV1066 effectively diagnosed peritoneal carcinomatosis by its EGFP expression of infected cells visible through a minimally invasive, laparoscopic system with appropriate fluorescent filters. After intraperitoneal administration of NV1066, macroscopic tumor foci that expressed EGFP were imaged by direct laparoscopy, whereas noncancerous organs were uninfected and did not express EGFP. EGFP expression in intraperitoneal tumors targeted by OV was visualized laparoscopically and allowed localization of tumors as well as tracking of viral gene therapy. Moreover, in another study, this fluorescent-guided tracking of NV1066 infection of peritoneal tumors informed real-time visualization of the residual tumor after attempted cytoreductive surgery and decreased minimal residual disease when FI was used to guide resection.[44] It was concluded that FI could be used to track viral infection for real-time intraoperative guidance in cytoreductive surgery to ensure completeness of resection and improve the oncologic quality of the operation.

Undoubtedly, preclinical studies suggest that tumor-targeted FI can be used for tracking OV therapy, improved cancer staging, and real-time surgical guidance to improve cancer surgery. The use of fluorescence to track OV therapy is undergoing initial testing in

Table 5. Clinical trials using optical imaging through gene therapy

Clinical trial	Disease process	Delivery route	Imaging modality	Clinical trial number
Phase 1	head and neck	i.v.	fluorescence microscopy and imaging	ClinicalTrials.gov: NCT01584284
Phase 1	solid tumor	i.v.	fluorescence microscopy	closed
Phase 1	recurrent ovarian	i.v.	fluorescence microscopy	ClinicalTrials.gov: NCT02759588
Phase 1	peritoneal carcinomatosis	i.p.	fluorescence microscopy	ClinicalTrials.gov: NCT01443260
Phase 2	recurrent ovarian	i.p.	fluorescence microscopy	ClinicalTrials.gov: NCT02759588

Only one oncolytic virus with optical imaging has reached clinical testing. This is the vaccinia virus Olvi-Vec (Genelux, San Diego, CA, USA). It carries the GFP gene for fluorescent imaging. The trials ongoing with this vector are listed. i.v., intravenous; i.p., intraperitoneal.

man. Fluorescence expressing OVs will likely be used as both a neo-adjuvant therapy for cancer as well as a potential tool for identifying small or occult tumors to enhance subsequent surgical resections of cancer.

CLINICAL TRIALS USING GENE THERAPY-BASED OPTICAL IMAGING

Staging of cancer

Patients with peritoneal dissemination of pancreatic adenocarcinoma do not benefit from surgical resection. Therefore, detection of peritoneal metastases is an essential part of staging patients. Kelly et al.[45] sought to determine if a fluorescent HSV that is highly specific for cancer can be used to allow sensitive detection of peritoneal disease. These investigators had determined that as few as 1 cancer cell in 2,000,000 normal cells can be detected by such fluorescence detection (Figure 2). Peritoneal washings from patients with pancreatic adenocarcinoma were incubated with the EGFP-expressing oncolytic HSV NV1066. EGFP-positive or -negative status was recorded for comparison to conventional cytology and to recurrence and survival for patients who underwent R0 resection. Of 82 patients entered in this trial, 12 (15%) had positive cytology, and 50 (61%) had virally mediated EGFP-positive cells in peritoneal washings. All cytology-positive patients were also EGFP positive. For detection of any peritoneal metastatic disease, HSV-mediated fluorescence detection had 100% sensitivity. Median recurrence-free and disease-specific survival was 6.5 and 18.3 months for EGFP-positive patients, versus 12.2 and 36.2 months for EGFP-negative patients (p = 0.01 and 0.19). This genetically modified HSV can be used as a highly sensitive optical diagnostic agent for detection of micro-metastatic disease in patients with pancreatic adenocarcinoma.

Tracking of gene therapy

Olvimulogene nanivacirepvec (GL-ONC1 or Olvi-Vec; Genelux, San Diego, CA, USA) is an attenuated oncolytic vaccinia virus encoding the light-emitting fusion protein Renilla luciferase-Aequorea GFP (RUC-GFP) with potential bioluminescent and antineoplastic activities.

Olvi-Vec has progressed through phases I and II clinical trials in treating multiple malignancies (Table 5). Olvi-Vec has been used to treat chemotherapy-refractory or recurrent ovarian cancer in phase I trials (ClinicalTrials.gov: NCT02759588).[46] A subsequent phase II expansion trial entitled VIRO-15 (ClinicalTrials.gov: NCT02759588) enrolled women with platinum-resistant or refractory ovarian cancer and sought to determine progression-free survival (PFS) and overall response rate (ORR) by imaging and CA-125. Patients were treated with carboplatin doublet with and without bevacizumab in addition to Olvi-Vec. Median PFS was 11.6 months, and ORR was 63%, with 5% of patients having a complete response. AEs were similar to the phase I trial, which included pyrexia (58%), abdominal pain (50%), nausea (50%), abdominal distension (46%), and fatigue (35%). Despite the AEs experienced in most of the cohort, performance status was preserved or improved in 92% of the participants. PFS and overall survival were improved compared to historical trials.[47]

At present, it is the only OV or cancer gene therapy capable of optical imaging that has entered human trials.[48] In two trials, the FI capabilities were put to use. The first was in a phase I trial of intraperitoneal viral delivery for advanced-stage peritoneal carcinomatosis or advanced peritoneal mesothelioma. Dose-limiting toxicity (DLT) was not reported, and the maximum tolerated dose (MTD) was not reached. Signs of viral shedding were not observed. Importantly, in 8 of 9 study patients, effective intraperitoneal infections, in-patient replication of GL-ONC1, and subsequent oncolysis were demonstrated in cycle 1.[49] As a correlative in this study, the investigators used fluorescent microscopy to examine peritoneal cells and were able to document viral replication by seeing increasing fluorescence over time.[49]

In the second trial, Olvi-Vec was also tested in an intravenous administration trial (ClinicalTrials.gov: NCT01584284) in addition to chemoradiation in patients with primary, non-metastatic, p16-positive oropharyngeal cancers. Nineteen stage IV patients were enrolled in 5 cohorts and treated with up to 3×10^9 plaque-forming units (PFUs) on days 3, 8, 15, and 22. Common AEs included rigors (68%), pyrexia (53%), fatigue (89%), and nausea (89%). In this trial, when skin rash occurred in 37% of patients, FI was used to confirm GFP expression at the pox-like lesion (Figure 3). The use of FI allows correlation of viral presence.[50]

Conclusions

Optical imaging is non-invasive, easy to use, and open to ready technologic advancements with the potential to impact preclinical design

Figure 3. Assessment of pox lesion during gene therapy with GL-ONC1 (Olvi-Vec), a vaccinia oncolytic virus expressing the GFP gene

The patient developed these pox lesions during treatment with GL-ONC1 + cisplatin + radiation therapy (XRT) for head and neck cancer (protocol ClinicalTrials.gov: NCT01584284). Pustules billed as "transient pox-like rash confirming systemic viral delivery" were confirmed as viral in origin by viral plaque assay (VPA) and fluorescence imaging; from Mell et al.[50] Reprinted from Clinical Cancer Research, 2017, 23/19, 5696-5702, Loren K Mell et al., Phase I Trial of Intravenous Oncolytic Vaccinia Virus (GL-ONC1) with Cisplatin and Radiotherapy in Patients with Locoregionally Advanced Head and Neck Carcinoma, with permission from AACR.

and clinical outcomes of cancer therapies significantly. BLI techniques will likely remain in the realm of laboratory and preclinical studies. FI is already in trials and clinics. To optimize each aspect of the FI techniques, efforts in this field have relied on GFP, ICG, novel fluorescent probes, and novel viruses carrying transgenes coding GFP. No doubt, exciting trials currently underway will result in future tools for tumor-specific optical imaging in cancer diagnostics and therapeutics.

ACKNOWLEDGMENTS

AUTHOR CONTRIBUTIONS

Y.W. and Y.F. conceived the manuscript. Y.W., S.C., M.O., E.H., and Y.F. collected related references and drafted the manuscript. Y.F. revised the manuscript. All authors read and approved the manuscript.

DECLARATION OF INTERESTS

Y.F. is a paid scientific consultant for Medtronics, Johnson & Johnson, Boehringer Ingelheim, and Imugene. Y.F. receives royalties for inventions from Merck and Imugene. All other authors have no competing interests.

REFERENCES

1. Wang, R.E., Zhang, Y., Tian, L., Cai, W., and Cai, J. (2013). Antibody-based imaging of HER-2: moving into the clinic. Curr. Mol. Med. 13, 1523–1537.

2. Vento, J., Mulgaonkar, A., Woolford, L., Nham, K., Christie, A., Bagrodia, A., de Leon, A.D., Hannan, R., Bowman, I., McKay, R.M., et al. (2019). PD-L1 detection using 89Zr-atezolizumab immuno-PET in renal cell carcinoma tumorgrafts from a patient with favorable nivolumab response. J. Immunother. Cancer 7, 144.

3. McCann, T.E., Kosaka, N., Choyke, P.L., and Kobayashi, H. (2012). The use of fluorescent proteins for developing cancer-specific target imaging probes. Methods Mol. Biol. 872, 191–204.

4. Bhaumik, S., and Gambhir, S.S. (2002). Optical imaging of Renilla luciferase reporter gene expression in living mice. Proc. Natl. Acad. Sci. USA 99, 377–382.

5. Barnes, T.G., Hompes, R., Birks, J., Mortensen, N.J., Jones, O., Lindsey, I., Guy, R., George, B., Cunningham, C., and Yeung, T.M. (2018). Methylene blue fluorescence of the ureter during colorectal surgery. Surg. Endosc. 32, 4036–4043.

6. Schebesch, K.M., Brawanski, A., Hohenberger, C., and Hohne, J. (2016). Fluorescein Sodium-Guided Surgery of Malignant Brain Tumors: History, Current Concepts, and Future Project. Turk Neurosurg. 26, 185–194.

7. Gioux, S., Choi, H.S., and Frangioni, J.V. (2010). Image-guided surgery using invisible near-infrared light: fundamentals of clinical translation. Mol. Imaging 9, 237–255.

8. Benya, R., Quintana, J., and Brundage, B. (1989). Adverse reactions to indocyanine green: a case report and a review of the literature. Cathet. Cardiovasc. Diagn. 17, 231–233.

9. Prasher, D.C., Eckenrode, V.K., Ward, W.W., Prendergast, F.G., and Cormier, M.J. (1992). Primary structure of the Aequorea victoria green-fluorescent protein. Gene 111, 229–233.

10. Sajedi, S., Sabet, H., and Choi, H.S. (2019). Intraoperative biophotonic imaging systems for image-guided interventions. Nanophotonics 8, 99–116.

11. van Manen, L., Handgraaf, H.J.M., Diana, M., Dijkstra, J., Ishizawa, T., Vahrmeijer, A.L., and Mieog, J.S.D. (2018). A practical guide for the use of indocyanine green and methylene blue in fluorescence-guided abdominal surgery. J. Surg. Oncol. 118, 283–300.

12. Morales-Conde, S., Alarcón, I., Yang, T., Licardie, E., Camacho, V., Aguilar Del Castillo, F., and Balla, A. (2020). Fluorescence angiography with indocyanine green (ICG) to evaluate anastomosis in colorectal surgery: where does it have more value? Surg. Endosc. 34, 3897–3907.

13. Shen, J.K., Jamnagerwalla, J., Yuh, B.E., Bassett, M.R., Chenam, A., Warner, J.N., Zhumkhawala, A., Yamzon, J.L., Whelan, C., Ruel, N.H., et al. (2019). Real-time indocyanine green angiography with the SPY fluorescence imaging platform decreases benign ureteroenteric strictures in urinary diversions performed during radical cystectomy. Ther. Adv. Urol. 11, 1756287219839631.

14. Sun, Z., Jing, L., Fan, Y., Zhang, H., Chen, L., Wang, G., Sharma, H.S., and Wang, J. (2020). Fluorescein-guided surgery for spinal gliomas: Analysis of 220 consecutive cases. Int. Rev. Neurobiol. 151, 139–154.

15. Cavallo, C., De Laurentis, C., Vetrano, I.G., Falco, J., Broggi, M., Schiariti, M., Ferroli, P., and Acerbi, F. (2018). The utilization of fluorescein in brain tumor surgery: a systematic review. J. Neurosurg. Sci. 62, 690–703.

16. Hillary, S.L., Guillermet, S., Brown, N.J., and Balasubramanian, S.P. (2018). Use of methylene blue and near-infrared fluorescence in thyroid and parathyroid surgery. Langenbecks Arch. Surg. 403, 111–118.

17. Spinoglio, G., Bertani, E., Borin, S., Piccioli, A., and Petz, W. (2018). Green indocyanine fluorescence in robotic abdominal surgery. Updates Surg. 70, 375–379.

18. Kwon, I.G., Son, T., Kim, H.I., and Hyung, W.J. (2019). Fluorescent Lymphography-Guided Lymphadenectomy During Robotic Radical Gastrectomy for Gastric Cancer. JAMA Surg. 154, 150–158.

19. Gentileschi, S., Servillo, M., Albanese, R., De Bonis, F., Tartaglione, G., and Salgarello, M. (2017). Lymphatic mapping of the upper limb with lymphedema before lymphatic supermicrosurgery by mirroring of the healthy limb. Microsurgery 37, 881–889.

20. Smith, B.L., Gadd, M.A., Lanahan, C.R., Rai, U., Tang, R., Rice-Stitt, T., Merrill, A.L., Strasfeld, D.B., Ferrer, J.M., Brachtel, E.F., and Specht, M.C. (2018). Real-time, intraoperative detection of residual breast cancer in lumpectomy cavity walls using a novel

cathepsin-activated fluorescent imaging system. Breast Cancer Res. Treat. *171*, 413–420.

21. Suurs, F.V., Qiu, S.Q., Yim, J.J., Schröder, C.P., Timmer-Bosscha, H., Bensen, E.S., Santini, J.T., Jr., de Vries, E.G.E., Bogyo, M., and van Dam, G.M. (2020). Fluorescent image-guided surgery in breast cancer by intravenous application of a quenched fluorescence activity-based probe for cysteine cathepsins in a syngeneic mouse model. EJNMMI Res. *10*, 111.

22. Miampamba, M., Liu, J., Harootunian, A., Gale, A.J., Baird, S., Chen, S.L., Nguyen, Q.T., Tsien, R.Y., and González, J.E. (2017). Sensitive *in vivo* Visualization of Breast Cancer Using Ratiometric Protease-activatable Fluorescent Imaging Agent, AVB-620. Theranostics *7*, 3369–3386.

23. Bradbury, M.S., Pauliah, M., Zanzonico, P., Wiesner, U., and Patel, S. (2016). Intraoperative mapping of sentinel lymph node metastases using a clinically translated ultrasmall silica nanoparticle. Wiley Interdiscip. Rev. Nanomed. Nanobiotechnol. *8*, 535–553.

24. Baik, F.M., Hansen, S., Knoblaugh, S.E., Sahetya, D., Mitchell, R.M., Xu, C., Olson, J.M., Parrish-Novak, J., and Méndez, E. (2016). Fluorescence Identification of Head and Neck Squamous Cell Carcinoma and High-Risk Oral Dysplasia With BLZ-100, a Chlorotoxin-Indocyanine Green Conjugate. JAMA Otolaryngol. Head Neck Surg. *142*, 330–338.

25. Zanzonico, P., Carrasquillo, J.A., Pandit-Taskar, N., O'Donoghue, J.A., Humm, J.L., Smith-Jones, P., Ruan, S., Divgi, C., Scott, A.M., Kemeny, N.E., et al. (2015). PET-based compartmental modeling of (124)I-A33 antibody: quantitative characterization of patient-specific tumor targeting in colorectal cancer. Eur. J. Nucl. Med. Mol. Imaging *42*, 1700–1706.

26. Fallahi, B., Khademi, N., Karamzade-Ziarati, N., Fard-Esfahani, A., Emami-Ardekani, A., Farzanefar, S., Eftekhari, M., and Beiki, D. (2021). 99mTc-PSMA SPECT/CT Versus 68Ga-PSMA PET/CT in the Evaluation of Metastatic Prostate Cancer. Clin. Nucl. Med. *46*, e68–e74.

27. Bhatnagar, J., Heroman, W., Murphy, M., and Austin, G.E. (2002). Immunohistochemical detection of carcinoembryonic antigen in esophageal carcinomas: a comparison with other gastrointestinal neoplasms. Anticancer Res. *22*, 1849–1857.

28. de Geus, S.W., Boogerd, L.S., Swijnenburg, R.J., Mieog, J.S., Tummers, W.S., Prevoo, H.A., Sier, C.F., Morreau, H., Bonsing, B.A., van de Velde, C.J., et al. (2016). Selecting Tumor-Specific Molecular Targets in Pancreatic Adenocarcinoma: Paving the Way for Image-Guided Pancreatic Surgery. Mol. Imaging Biol. *18*, 807–819.

29. Gebauer, F., Wicklein, D., Horst, J., Sundermann, P., Maar, H., Streichert, T., Tachezy, M., Izbicki, J.R., Bockhorn, M., and Schumacher, U. (2014). Carcinoembryonic antigen-related cell adhesion molecules (CEACAM) 1, 5 and 6 as biomarkers in pancreatic cancer. PLoS ONE *9*, e113023.

30. Kim, J., Kaye, F.J., Henslee, J.G., Shively, J.E., Park, J.G., Lai, S.L., Linnoila, R.I., Mulshine, J.L., and Gazdar, A.F. (1992). Expression of carcinoembryonic antigen and related genes in lung and gastrointestinal cancers. Int. J. Cancer *52*, 718–725.

31. Park, S.-H., Ku, K.-B., Chung, H.-Y., and Yu, W. (2008). Prognostic significance of serum and tissue carcinoembryonic antigen in patients with gastric adenocarcinomas. Cancer Res. Treat. *40*, 16–21.

32. Hoogstins, C.E.S., Boogerd, L.S.F., Sibinga Mulder, B.G., Mieog, J.S.D., Swijnenburg, R.J., van de Velde, C.J.H., Farina Sarasqueta, A., Bonsing, B.A., Framery, B., Pèlegrin, A., et al. (2018). Image-Guided Surgery in Patients with Pancreatic Cancer: First Results of a Clinical Trial Using SGM-101, a Novel Carcinoembryonic Antigen-Targeting, Near-Infrared Fluorescent Agent. Ann. Surg. Oncol. *25*, 3350–3357.

33. Framery, B., Gutowski, M., Dumas, K., Evrard, A., Muller, N., Dubois, V., Quinonero, J., Scherninski, F., Pèlegrin, A., and Cailler, F. (2019). Toxicity and pharmacokinetic profile of SGM-101, a fluorescent anti-CEA chimeric antibody for fluorescence imaging of tumors in patients. Toxicol. Rep. *6*, 409–415.

34. Gutowski, M., Framery, B., Boonstra, M.C., Garambois, V., Quenet, F., Dumas, K., Scherninski, F., Cailler, F., Vahrmeijer, A.L., and Pèlegrin, A. (2017). SGM-101: An innovative near-infrared dye-antibody conjugate that targets CEA for fluorescence-guided surgery. Surg. Oncol. *26*, 153–162.

35. Yazaki, P., Lwin, T., Minnix, M., Li, L., Sherman, A., Molnar, J., Miller, A., Frankel, P., Chea, J., Poku, E., et al. (2019). Improved antibody-guided surgery with a near-infrared dye on a pegylated linker for CEA-positive tumors. J. Biomed. Opt. *24*, 1–9.

36. DeLong, J.C., Murakami, T., Yazaki, P.J., Hoffman, R.M., and Bouvet, M. (2017). Near-infrared-conjugated humanized anti-carcinoembryonic antigen antibody targets colon cancer in an orthotopic nude-mouse model. J. Surg. Res. *218*, 139–143.

37. Lwin, T.M., Murakami, T., Miyake, K., Yazaki, P.J., Shivley, J.E., Hoffman, R.M., and Bouvet, M. (2018). Tumor-Specific Labeling of Pancreatic Cancer Using a Humanized Anti-CEA Antibody Conjugated to a Near-Infrared Fluorophore. Ann. Surg. Oncol. *25*, 1079–1085.

38. Lwin, T.M., Miyake, K., Murakami, T., DeLong, J.C., Amirfakhri, S., Filemoni, F., Yoon, S.N., Yazaki, P.J., Shivley, J.E., Datnow, B., et al. (2018). Fluorescent humanized anti-CEA antibody specifically labels metastatic pancreatic cancer in a patient-derived orthotopic xenograft (PDOX) mouse model. Oncotarget *9*, 37333–37342.

39. Metildi, C.A., Kaushal, S., Pu, M., Messer, K.A., Luiken, G.A., Moossa, A.R., Hoffman, R.M., and Bouvet, M. (2014). Fluorescence-guided surgery with a fluorophore-conjugated antibody to carcinoembryonic antigen (CEA), that highlights the tumor, improves surgical resection and increases survival in orthotopic mouse models of human pancreatic cancer. Ann. Surg. Oncol. *21*, 1405–1411.

40. Adusumilli, P.S., Eisenberg, D.P., Stiles, B.M., Chung, S., Chan, M.K., Rusch, V.W., and Fong, Y. (2006). Intraoperative localization of lymph node metastases with a replication-competent herpes simplex virus. J. Thorac. Cardiovasc. Surg. *132*, 1179–1188.

41. Stanziale, S.F., Stiles, B.M., Bhargava, A., Kerns, S.A., Kalakonda, N., and Fong, Y. (2004). Oncolytic herpes simplex virus-1 mutant expressing green fluorescent protein can detect and treat peritoneal cancer. Hum. Gene Ther. *15*, 609–618.

42. Gil, Z., Cavel, O., Kelly, K., Brader, P., Rein, A., Gao, S.P., Carlson, D.L., Shah, J.P., Fong, Y., and Wong, R.J. (2010). Paracrine regulation of pancreatic cancer cell invasion by peripheral nerves. J. Natl. Cancer Inst. *102*, 107–118.

43. Eisenberg, D.P., Adusumilli, P.S., Hendershott, K.J., Chung, S., Yu, Z., Chan, M.K., Hezel, M., Wong, R.J., and Fong, Y. (2006). Real-time intraoperative detection of breast cancer axillary lymph node metastases using a green fluorescent protein-expressing herpes virus. Ann. Surg. *243*, 824–830, discussion 830–832.

44. Adusumilli, P.S., Eisenberg, D.P., Chun, Y.S., Ryu, K.W., Ben-Porat, L., Hendershott, K.J., Chan, M.K., Huq, R., Riedl, C.C., and Fong, Y. (2005). Virally directed fluorescent imaging improves diagnostic sensitivity in the detection of minimal residual disease after potentially curative cytoreductive surgery. J. Gastrointest. Surg. *9*, 1138–1146, discussion 1146–1147.

45. Kelly, K.J., Wong, J., Gönen, M., Allen, P., Brennan, M., Coit, D., and Fong, Y. (2016). Human Trial of a Genetically Modified Herpes Simplex Virus for Rapid Detection of Positive Peritoneal Cytology in the Staging of Pancreatic Cancer. EBioMedicine *7*, 94–99.

46. Holloway, R.W., Kendrick, J.E., Stephens, A., Kennard, J., Burt, J., LeBlanc, J., Sellers, K., Smith, J., and Coakley, S. (2018). Phase 1b study of oncolytic vaccinia virus GL-ONC1 in recurrent ovarian cancer (ROC). J. Clin. Oncol. *36*, 5577.

47. Holloway, R.W., Mendivil, A.A., Kendrick, J.E., Abaid, L.N., Brown, J.V., Fitzsimmons, C.K., Kennard, J.A., King, M.M., LeBlanc, J., Lopez, K., et al. (2020). Phase II VIRO-15 trial of olvimulogene nanivacirepvec (Olvi-Vec)-primed immuno-chemotherapy in platinum-resistant/refractory ovarian cancer (PRROC) (NCT02759588). Gynecol. Oncol. *159*, 60.

48. Zhang, Q., Yu, Y.A., Wang, E., Chen, N., Danner, R.L., Munson, P.J., Marincola, F.M., and Szalay, A.A. (2007). Eradication of solid human breast tumors in nude mice with an intravenously injected light-emitting oncolytic vaccinia virus. Cancer Res. *67*, 10038–10046.

49. Lauer, U.M., Schell, M., Beil, J., Berchtold, S., Koppenhöfer, U., Glatzle, J., Königsrainer, A., Möhle, R., Nann, D., Fend, F., et al. (2018). Phase I Study of Oncolytic Vaccinia Virus GL-ONC1 in Patients with Peritoneal Carcinomatosis. Clin. Cancer Res. *24*, 4388–4398.

50. Mell, L.K., Brumund, K.T., Daniels, G.A., Advani, S.J., Zakeri, K., Wright, M.E., Onyeama, S.J., Weisman, R.A., Sanghvi, P.R., Martin, P.J., and Szalay, A.A. (2017). Phase I Trial of Intravenous Oncolytic Vaccinia Virus (GL-ONC1) with Cisplatin and Radiotherapy in Patients with Locoregionally Advanced Head and Neck Carcinoma. Clin. Cancer Res. *23*, 5696–5702.